Chapter 2

Fabrication and Characterization of ZnO CQDs/ TIPS-Pentacene Heterojunction based UV-Visible Photodetector

***Part of this work has been published as:**

Abhinav Pratap Singh, R. K. Upadhyay, and S. Jit, "High-Performance Colloidal ZnO Quantum Dots / TIPS-Pentacene Heterojunction Based Ultraviolet Photodetector," ***IEEE Transactions on Electron Devices*****,** pp. 1–6, **2022**, DOI: 10.1109/TED.2022.3166120.

Chapter 2

Fabrication and Characterization of ZnO CQDs/ TIPS-Pentacene Heterojunction based UV-Visible Photodetector

2.1 Introduction

Photodetectors are generally classified on the detection range of wavelength of radiation or photo. Among various photodetectors, ultraviolet (UV) photodetectors have drawn considerable attention for advanced communications, flame detection, air purification, ozone sensing and leak detection, missile tracking and missile plume detection, environment monitoring, chemical-biological analysis, water purification, etc. [64]. The performance parameters of photodetectors (including UV photodetectors) primarily depend on the semiconductor materials and device's structure. The advantage of organic semiconductors and heterojunction structure is already discussed in Chapter-1. Some solution processed metal oxides and their nanostructures are found compatible for the organic based heterojunction photodetectors. One of widely used metal oxide for photodetection application is Zinc oxide (ZnO). ZnO has excellent UV photodetection characteristics due to its inherently large direct bandgap energy of ~3.37 eV, low-cost and low-temperature processing, strong radiation hardness, high chemical stability and environment-friendly nature [6], [7]. As discussed in previous chapter, the quantum dots have exhibited relatively better optoelectronic properties owing to their high surface to volume ratio and enhanced carrier confinement nature. Therefore, colloidal quantum dots (CQDs) of ZnO, which has size-dependent absorption tuning capability, are largely used in UV photodetection [7].

For the fabrication of heterojunction photodetectors, ZnO is widely used with organic semiconductors namely poly(N-vinyl carbazole) (PVK) [29], Poly (3-hexylthiophene-2, 5-diyl) (P3HT), Poly (9, 9- dihexylfluorene) (PFH) [65], and pentacene [6]-[68]. Among various organic semiconductors, pentacene is considered to be a very promising organic semiconductor for UV photodetectors due to its high carrier mobility and air-stability [68]. However, the poor solubility of the pentacene with various organic solvents makes it difficult to fabricate the low-cost, low-temperature and large area solution-processed photodetectors. In this regard, the 6, 13-bis (tri-isopropyl-silylethynyl) (TIPS)-Pentacene could be a better choice alternative due to its better solubility in organic solvents, higher carrier mobility and improved air-stability over the pentacene films [69]–[71]. Further, the TIPS-Pentacene shows a tendency for singlet fission (SF) that may enable photodetection with >100% external quantum efficiency [72]. Thus, the performance of n-ZnO CQDs/p-TIPS-Pentacene heterojunction UV photodetector is expected to be enhanced by the combined absorptions in both the materials as well as the spectrum selective UV absorption property of the ZnO CQDs.

In this chapter, we propose an n-ZnO colloidal quantum dots (CQDs) and p-TIPS-pentacene thin films based heterojunction UV photodetector fabricated by the low-cost solution method on an ITO coated glass substrate. In brief the section 2.1 covers the key experimental details followed by result and discussion section (2.2) which includes a detailed analysis of optoelectronic characterization, performance parameter extraction and brief discussion of the obtained result. This is followed by a conclusion in section 2.4, which summarizes the result outcome and performance enhancement mechanism.

2.2 Experimental Details

2.2.1. Preparation of colloidal ZnO CQDs

Quantum dots or zero-dimensional materials are finding increased attention in optoelectronic devices owing to their large surface-to-volume ratio and quantum confinement nature. Moreover, the bandgap of material can easily be tuned by varying the size of Quantum dots thereby targeting broadband for photodetector. It is the quantum confinement property that sets apart the 0-D materials from their bulk counterparts. However, in order to achieve quantum confinement, the size of the nanoparticle should be smaller than the Bohr exciton radius. Therefore, the control sized ZnO QDs have been synthesized by hot injection route previously reported in ref. [73] with slightly modified experimental setup as shown in Figure 2.1. In this process, zinc-acetate dihydrate (Sigma-Aldrich, 99.99%, 500mM) precursor was dissolved in ethylene glycol monomethyl ether (Sigma-Aldrich, 99.99%, 20mL) as coordinating ligand in a three-neck flask under a nitrogen environment. The solution was stirred continuously and its temperature was gradually increased and then was maintained at 60°C. When the mixed solution became a transparent one, the monoethanolamine (MEA) (Sigma-Aldrich, 99.99%) as the reagent of the equal-molar ratio was then swiftly injected into the solution to obtain ZnO CQDs by nucleation of ZnO particles [74].

2.2.2. Fabrication of Photodetector

The ITO coated glass substrates (15mm x 15mm) were cleaned in a 1:6 ratio of soap solution and deionized (DI) water ultra-sonically for 20 minutes, followed by rinsing for 10 minutes in fresh DI water. The substrates were cleaned ultrasonically with acetone and isopropanol

for 20 minutes and then finally in an Argon plasma (using Femto Science Inc. CUTE, Korea) [75]. The as-synthesized ZnO CQDs are spin-coated on the substrates at 2000 rpm for 40 sec (using SPM-150LC TSE-system GmbH, Germany). The ZnO CQDs film was then dried at 120° C for 10 minutes on a hot plate in an ambient environment. The process was repeated to get desired ZnO QDs thickness of ~200 nm (measured by using reflectometer, F-20 Filmetrics). The ZnO QDs film was finally annealed at 450° C for 30 minutes in a muffle furnace under an ambient environment. Separately, the solution of TIPS-pentacene was prepared by dissolving the TIPS-pentacene (Ossila Limited, U.K.) in dichlorobenzene solution (10 mg/mL). The TIPS-pentacene film was developed on the ZnO QDs film by spin coating at 1500 rpm for 30 s. The TIPS-pentacene film (~120 nm thickness) was then dried at 100°C in a prebake oven under an N_2 gas environment for 60 min. Finally, the top contact electrode of silver (Ag) metal (99.99%) dots of 1 mm radius (with an effective area of the device as 0.0314 cm^2 [76]) and ~120 nm thickness were grown by a thermal evaporation method (FL400 SMART COAT 3.0 A, Hind High Vacuum, India) at a high vacuum of ~0.22×10^{-6} mbar and ~0.2 nm/s deposition rate. Since Ag is cheaper than other commonly used noble metals such as Au, Pd and Pt, so Ag Ag electrode is used to reduce the fabrication cost of the device.

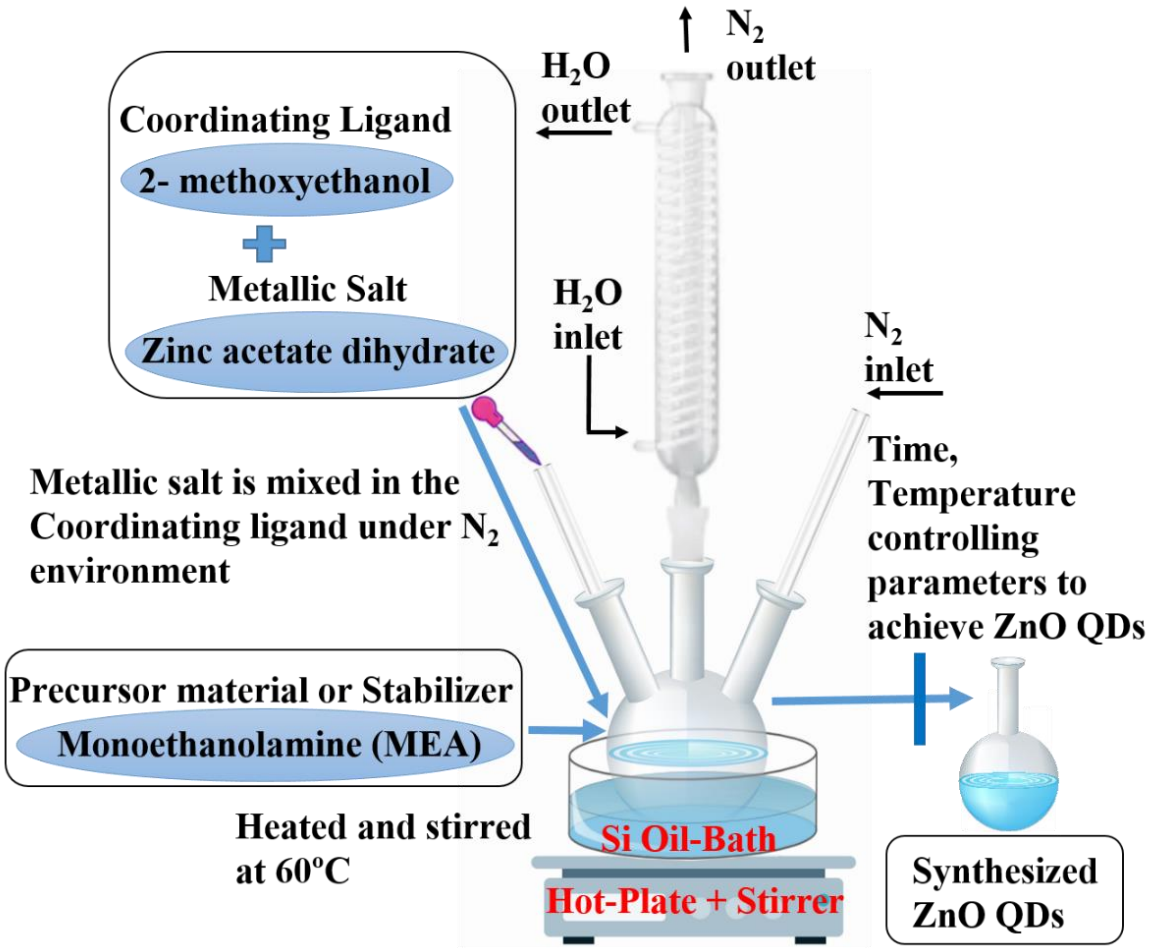

Figure 2.1: Experimental setup with specifications and steps for solution synthesis of colloidal quantum dots using hot injection method.

2.3. Results And Discussion

2.3.1. Structural Characterization of as-grown ZnO CQD

The surface of ZnO CQDs is characterized using transmission electron microscopy (TEM, from TECNAI G2 20 TWIN) image of the ZnO CQDs film deposited on a copper grid. TEM images at 20 nm and 50 nm resolutions are shown in Figure 2.2. The particle size distribution of the ZnO QDs is characterized by the histogram as shown in Figure 2.3 (a). The TEM image shows the nanoparticle nature of the ZnO in the solution. The histogram

shows an average particle size of ~2.00 nm. The average particle size of the ZnO particles below the value of the Bohr's radius of ~2.87 nm of the ZnO confirms the QDs nature of ZnO nanoparticles in the ZnO solution prepared by the hot injection method as reported in [63].

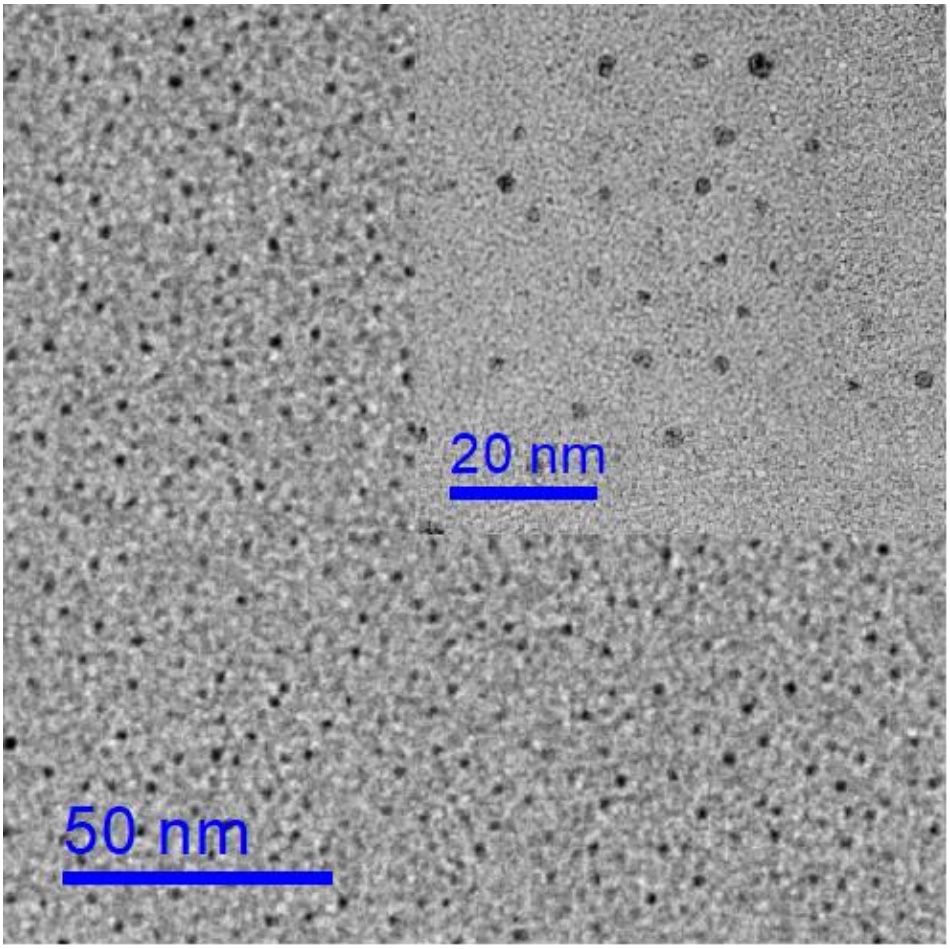

Figure 2.2: TEM image of ZnO QDs at 50nm scale resolution [inset with a scale resolution of 20nm].

The selected area electron diffraction (SAED) image of ZnO QDs is shown in Figure 2.3 (b). The diffused concentric rings are continuous in the SAED image, confirming that the particle size of the material is very small. As a result, the nature of the QDs is single crystalline with a large surface to volume ratio. Using the Crystallography Open Database (COD) number 2300112, the *d*-spacing of ZnO QDs is determined to be 0.262 nm and 0.146 nm corresponding to the orientations of <002> and <103>, respectively [77][78].

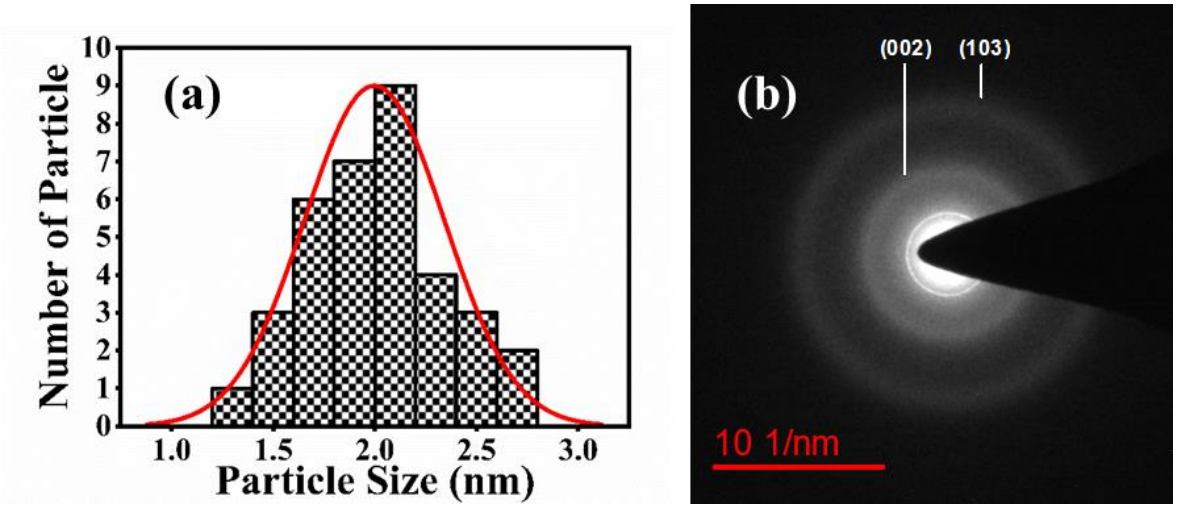

Figure 2.3: (a) Histogram of ZnO QD and (b) SAED image of ZnO QD.

2.3.2. Steady State Absorption and Photoluminescence Analysis of Thin Film

The UV-Vis spectroscopic measurements (V-770 from JASCO, Japan) have been used to obtain the absorption characteristics of the ZnO CQDs, TIPS-pentacene and ZnO CQDs/TIPS-pentacene structure as shown in Figure 2.4 (a). It is observed that both the ZnO CQDs and TIPS-Pentacene have wide absorption characteristics covering both the UV and visible regions. The ZnO CQDs/TIPS-Pentacene heterojunction thus shows improved absorption over the individual absorptions of the ZnO CQDs and TIPS-Pentacene films due to the combined absorption effects of the individual layers in the fabricated heterojunction device.

The corresponding photoluminescence (PL) of the ZnO CQDs, TIPS-Pentacene and ZnO CQDs/ TIPS-Pentacene device measured at the excitation wavelength (λ_{ex}) of 375 nm is shown in Figure 2.4 (b) with the help of Edinberg Spectrofluorometer FS980. The emission peak for the ZnO CQDs film appears at ~435 nm as shown in Figure 2.4 (b) (i). In contrast,

no emission is observed for sole TIPS-Pentacene film shown in Figure 2.4 (b) (ii). However, in the ZnO CQDs/ TIPS-Pentacene heterojunction, the fluorescence intensity of the ZnO CQDs has been decreased but the fluorescence intensity of the TIPS-Pentacene has appeared in Figure 2.4 (b) (iii) due to excitation energy transfer from the ZnO CQD to TIPS-Pentacene owing to the sufficient overlapping between the emission of ZnO CQD and absorption of TIPS-Pentacene.

2.3.3. Time-domain Fluorescence analysis of the thin film

To understand the mechanism of fluorescence quenching of ZnO CQDs and fluorescence enhancement of TIPS-Pentacene in the heterojunction device, the time-domain measurements of these sample films were carried out at 450 nm, 660 nm and 720 nm emission peaks for ZnO CQDs/TIPS-Pentacene. The fluorescence of ZnO CQD thin film is found best fitted in triple exponential decay function with decay times 0.84 ns, 4.0 ns and 13.59 ns having amplitude of 68%, 25% and 7%, respectively as shown in Figure 2.5 (i). In contrast, no decay profile was observed in the TIPS-Pentacene thin film due to no detectable fluorescence [79]. However, in the case of the ZnO CQDs/TIPS-Pentacene heterojunction, the fluorescence decay of ZnO CQD quenches at 450 nm [see Figure 2.5 (ii)], where no changes in the decay profiles of TIPS-Pentacene at 660 and 720 nm are observed in Figure 2.5 (iii) and (iv). Similar to the PL of ZnO CQDs [see Figure 2.4 (b) (iii)], the fluorescence decay time of long and short decay components is decreased

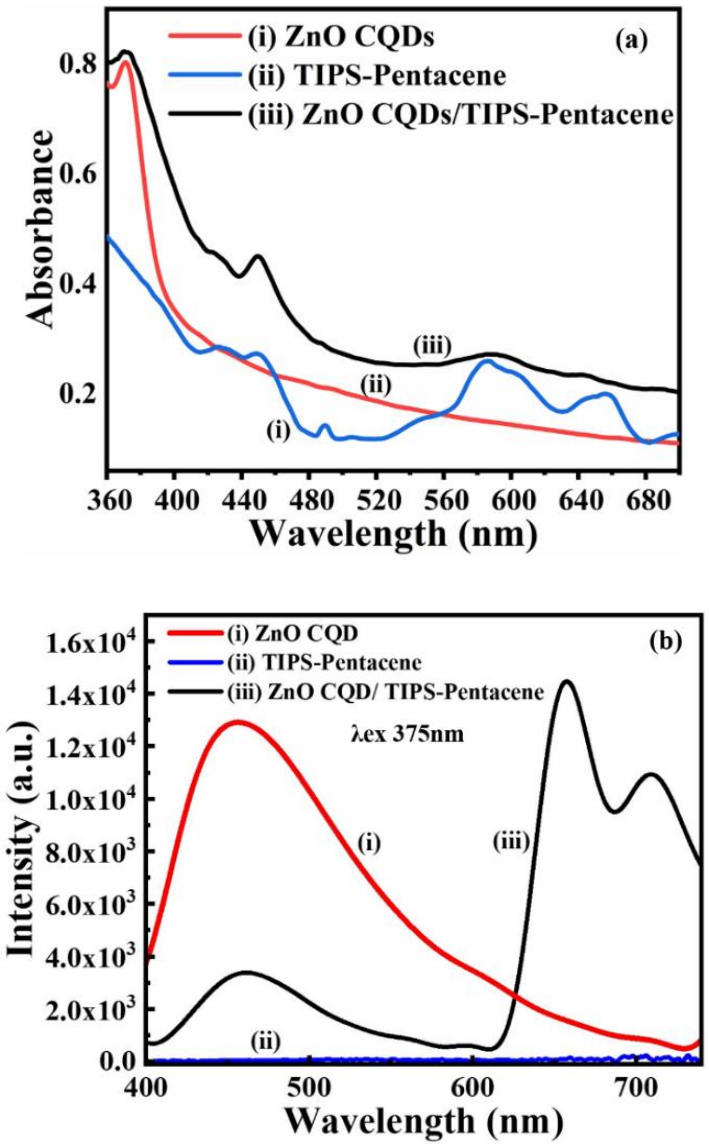

Figure 2.4 (a) Absorption spectra of the films under study, and (b) Emission spectra of (i) ZnO CQDs thin film, (ii) TIPS-Pentacene thin film, (iii) ZnO CQDs / TIPS-Pentacene heterostructure material.

from 13.59 ns to 1.96 ns and 0.84 ns to 0.52ns, respectively, in the presence of TIPS-Pentacene in the heterojunction thin-film. In comparison, no change in the third decay time of 4.0 ns is observed in the heterojunction film, which confirms the excitation energy transfer from ZnO- CQD to TIPS-Pentacene along with the excited-state electron transfer. This shows that the quenching of PL intensity and decay time of ZnO CQD is caused by both the excited state electron transfer and energy transfer from the ZnO CQDs to TIPS-Pentacene,

which is responsible for the enhancement of the PL intensity of the TIPS-Pentacene in Figure 2.4 (b) (iii).

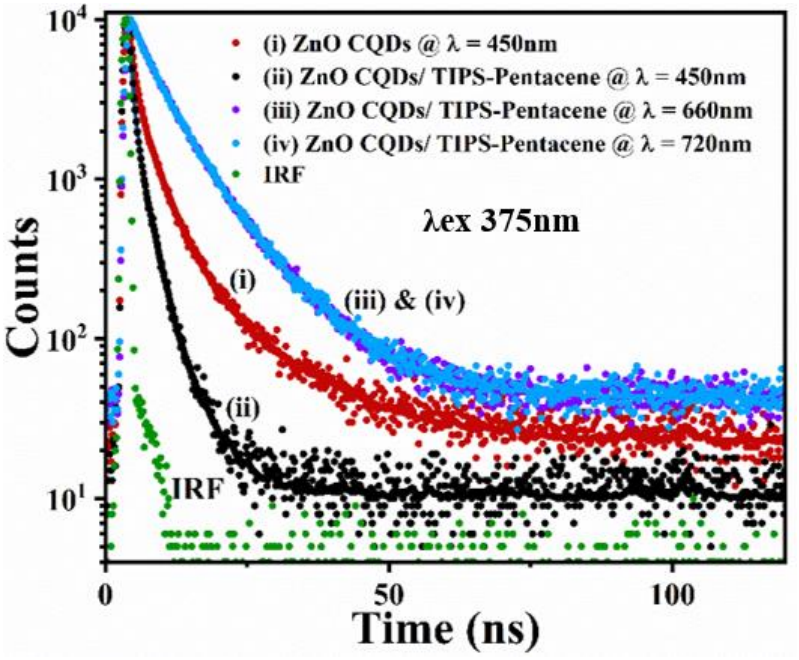

Figure 2.5 Fluorescence Decay curve of (i) ZnO CQDs thin film at λem=450nm, and ZnO CQDs / TIPS-Pentacene Device at (ii) λem 450nm, (iii) λem 660nm and (iv) λem 720nm (λex 375nm p-sec laser) with instrument response function (IRF).

2.3.4. Optoelectronics Characterization of Photodetector

Figure 2.6 (a) depicts the procedure required for the fabrication of the device, and the image of the fabricated device from the top view and back view along with electrode contacts are shown in Figure 2.6 (c). The band diagram of the device is shown in Figure 2.6 (b). The bandgap energy of ZnO CQDs is assumed 3.23 eV with its conduction band (CB) and valence band (VB) energies of 7.59 eV and 4.36 eV, respectively [80].

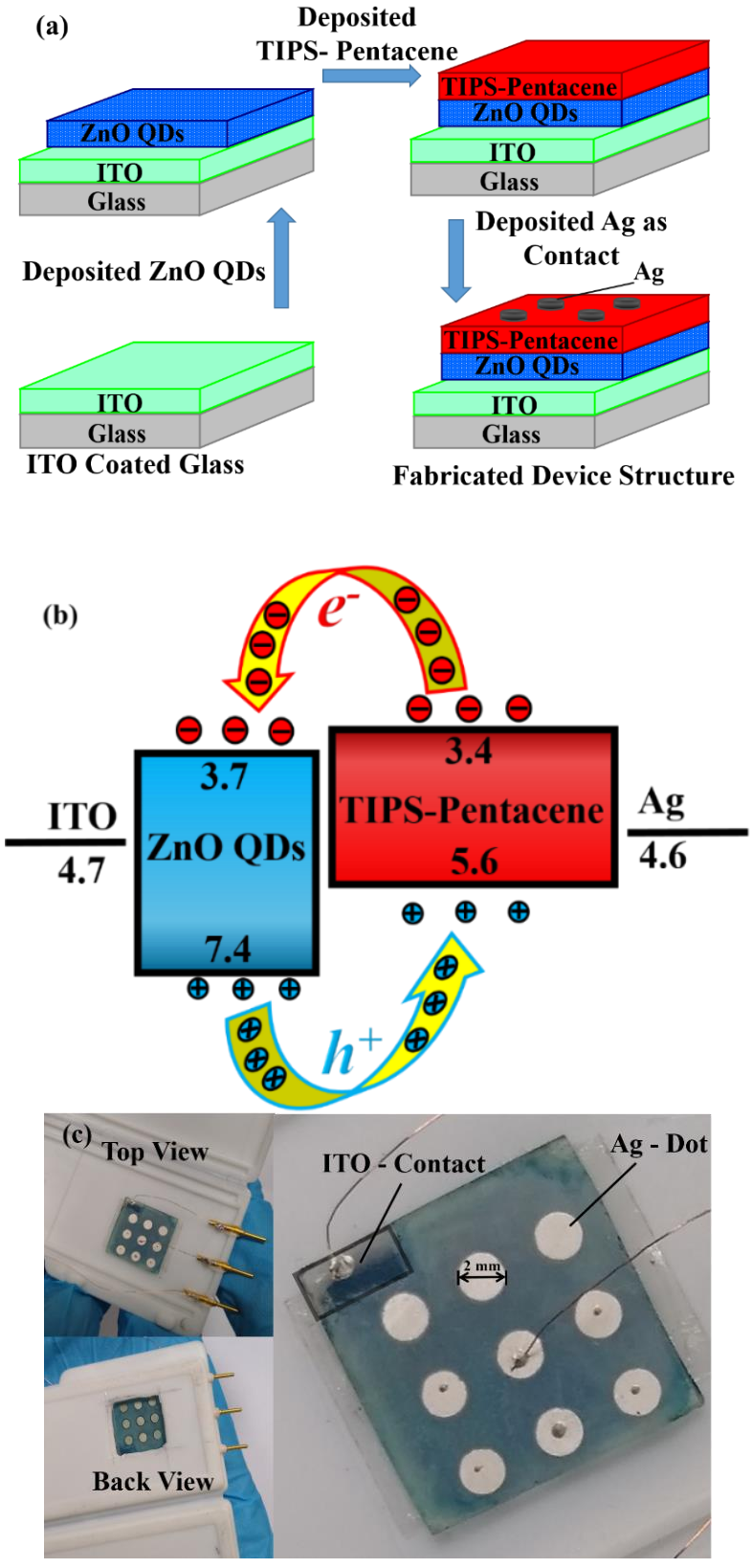

Figure 2.6 (a) Fabricated device structure, (b) Band diagram and (c) Fabricated Image of the device ITO/ZnO CQD/TIPS-Pentacene/Ag.

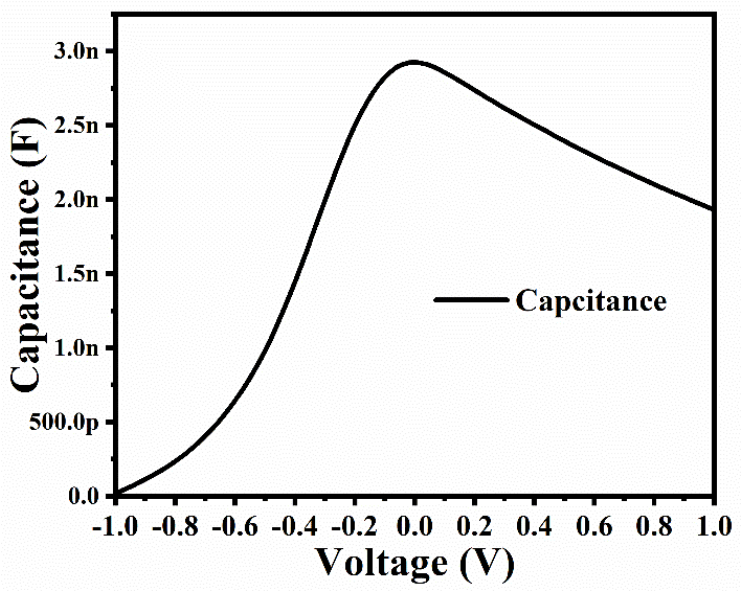

Figure 2.7 C-V characteristic of the fabricated device.

The bandgap of the TIPS-Pentacene is assumed to be 1.87 eV with VB=3.53 eV and CB=5.4 eV [18]. The Ag electrode with work function of 4.6 eV is used to make a good energy band alignment with the TIPS-Pentacene to facilitate easy movement of the holes toward this electrode. Further, ZnO CQD is used as an active cum electron transport layer and TIPS-Pentacene is used as a hole transport layer of the photodetector. The measured *C-V* characteristic at 1MHz frequency using a semiconductor parameter analyzer (B1500A from Keysight, USA) is shown in Figure 2.7. The decrease in the capacitance with increased reverse bias confirms the formation of the ZnO CQDs/TIPS-Pentacene heterojunction of the proposed device, and the current (*I*)-voltage (*V)* characteristics under dark and UV-illumination (370 nm) are compared in Figure 2.8. The asymmetric nature again confirms the p-n heterojunction formation of the device.

The responsivity and detectivity are shown in Figure 2.9, Resonsivity (R) is the photoresponse at a particular wavelength of incident light. It is generally expressed in A/W.

It is defined as the ratio of the generated photocurrent to the incident optical power at a given wavelength of incident light. The responsivity is expressed as:

$$R = \frac{\text{Change in Current / Effective Area of Device}}{\text{incident Power Density on the Device}} \quad (2.1)$$

The proposed device exhibits a very promising responsivity of ~59.15 A/W at ~370 nm UV light of ~43μW/cm^2 power density under 1 V reverse bias voltage due to the ZnO CQDs layer act as an active material in UV region and also works as ETL of the device. Note that the photoresponse at longer wavelengths occurs mainly by the absorption in the TIPS-Pentacene films and works as a HTL of the device. However, poor mobility of the carrier in polymer region results in very low absorption of photons at longer wavelengths. This perhaps results in poor responsivity at longer wavelengths but in UV region the responsivity is very promising as compare to the similar reported literature based on ZnO/polymer based photodetector in Table 2.1.

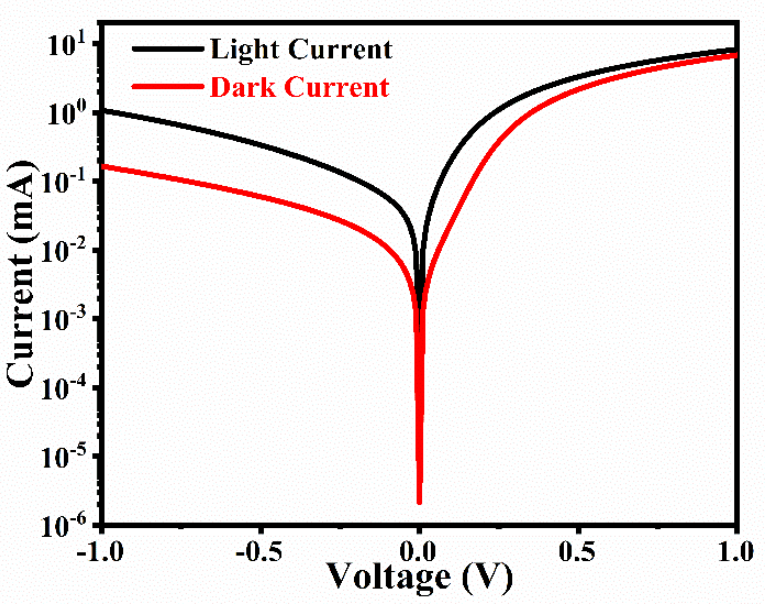

Figure 2.8 I-V characteristic of ITO/ZnO CQDs/TIPS-Pentacene/Ag.

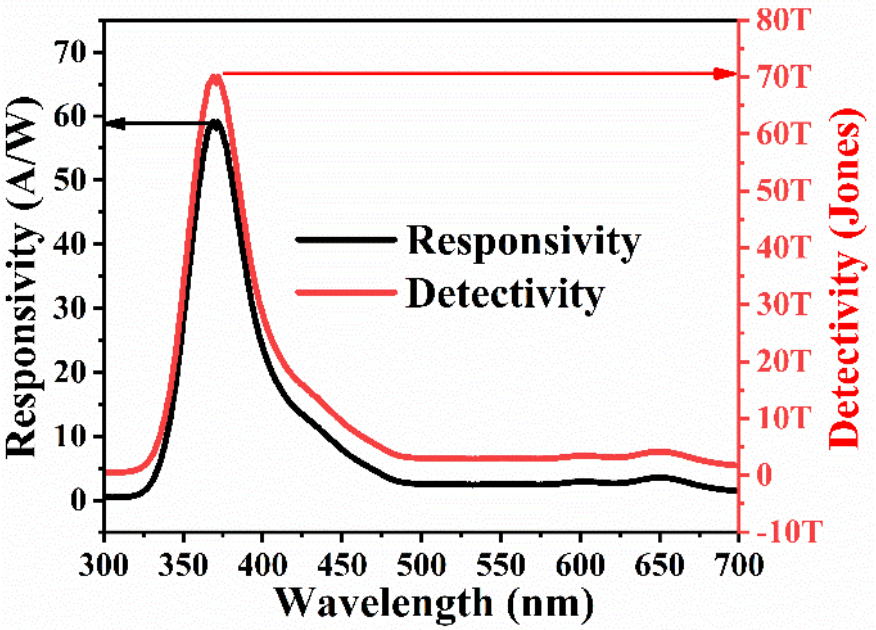

Figure 2.9 Responsivity and Detectivity characteristic of ITO/ZnO CQDs/TIPS-Pentacene/Ag.

The Detectivity is also an important parameter of the photodetector. It is the figure of merits to measure the performance of device in terms of the device noise and directly proportional to the responsivity of the device. The dark current is the major contribution of the noice. The detectivity (D^*) of the proposed device is calculated using the following equation [81],[82]:

$$D^* = \frac{R}{\sqrt{2 \times e^- \times J_d}} \qquad (2.2)$$

Where, R is responsivity, e^- is the charge of an electron, and J_d is the dark current density.

The device is found to exhibit a maximum detectivity (D^*) of ~ 7.01×10^{13} cmHz$^{1/2}$/W (or Jones) as shown in Fig. 2.9. The external quantum efficiency (EQE) is defined as the ratio of number of electrons-hole pairs collected at external terminal to the number of photons of a particular wavelength incident on the device. The EQE is expressed as

$$EQE\ \% = \frac{1240 \times R}{\lambda\,(nm)} \times 100 \qquad (2.3)$$

where, R is responsivity, and λ is the incident wavelength in nm. The device exhibits a promising EQE of ~19877 % at ~370 nm UV light of ~43μW/cm^2 power density and 1 V reverse bias voltage.

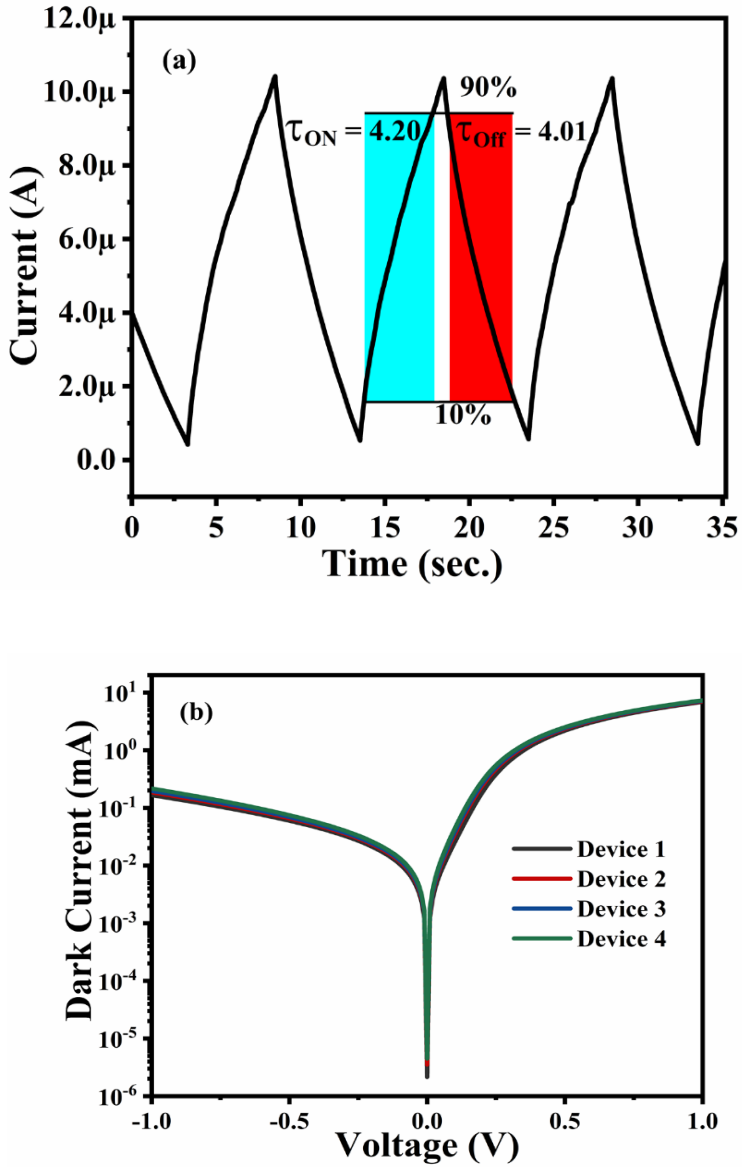

Figure 2.10 (a) Rise-time and fall-time of transient response characteristics of the device illuminated by 370 nm monochromator light source (optical power density ~13.6 μW/cm^2) at -1 V bias. (b). I-V characteristics (under dark condition) of 4 different devices fabricated under similar conditions to show the reproducibility of the proposed device.

This high EQE may be attributed to both the excited state electron transfer and energy transfer from the ZnO CQDs to TIPS-Pentacene in the heterostructure based active material of the device.

Finally, the transient response characteristics were measured in terms of rise-time (τ_r) (which is defined as the time for the pulse to rise from 10% to 90% of the final value) and fall-time (τ_f)

TABLE 2.1: COMPARISON OF RESPONSIVITY AND DETECTIVITY OF ZNO BASED PHOTODETECTORS

Device Structure	**R (AW^{-1})**	**D^* (Jones)**	**Reference**
ITO/ZNO CQDs/TIPS-Pentacene/Ag	59.15	7.01×10^{13}	This Work
FTO/ZnO-NR/PProDOT/ ZnO-NR/FTO	27.5	1.98×10^{12}	[83]
FTO/ZnO-NR/PProDOT-OH/ ZnO-NR/FTO	34.75	2.61×10^{12}	[83]
ITO/ZnO NR/P3HT/Au/PEDOT:PSS/ Ag	17.7	-	[27]
ITO/Cu2O/PVK/ZnO NR/Ag	13.28	1.03×10^{13}	[29]
ITO/ZnO NR/P3HT/PEDOT:PSS/Ag	10.7	-	[27]
e-GaIn /Si/ZnO/PEDOT: PSS/ Graphite	0.064	-	[84]
ITO/ZnO/PEDOT:PSS/Au	5.046	-	[30]
ITO/ZnO/PEDOT:PSS/Au	0.013	-	[85]

(defined as the time for the pulse to fall from 90% to 10% of the final value) by using a pulsed light of ~370 nm wavelength with an equal on-off time of 10 s and power density of ~13.6 $\mu W/cm^2$. Fig. 10 (a) shows the transient responses and rise-time and fall-time of 4.20 s and 4.01 s, respectively. The response times appear to be a bit high due to the low mobility of carriers in the high concentration or bulk of TIPS-Pentacene. Further, the fabrication and characterization of the proposed device in an open environment (without using any controlled condition, not even any cleanroom facility) may lead to the creation of some defects in the polymer as well as at the heterojunction interface. This could also lead to the poor speed of the device [86]. The large RC time constant may also limit the device speed [87]. However, the measured rise-time and fall-time of our proposed device are still better than many UV-Visible photodetectors ZnO and its nanostructures [86], [87]. To investigate the fabrication repeatability of the proposed photodetector, the dark current characteristics of four different devices 1,2,3, and 4 fabricated under similar environmental conditions are compared in Fig. 10 (b). Close matching in the I-V characteristics of all the four devices confirms that the proposed device is reproducible.

2.4. Conclusion

In this chapter our main objective was to fabricate an ITO/ZnO CQDs/TIPS-Pentacene/Ag structure-based heterojunction photodiode by utilizing a low-cost solution process. The heterojunction of organic semiconductor 6, 13-bis (tri-isopropyl-silylethynyl) (TIPS)-pentacene and ZnO CQDs is fabricated. TIPS-pentacene performed as an active material due its inherent properties such as better solubility in organic solvents, higher carrier mobility and improved air-stability over the other organic material like pristine pentacene. ZnO CQDs is synthesized by the hot-injection route show an average particle size of ~2.0

nm. The ZnO CQDs / TIPS-pentacene heterojunction shows excellent absorption characteristics in the UV region at ~ 370 nm. The heterojunction formation is confirmed by the C-V and I-V characteristics of the device. The device operated under a reverse bias voltage of 1 V exhibits the maximum responsivity, detectivity and EQE of ~59.15 A/W and ~ 7.01×10^{13} Jones, and ~19877 %, respectively at ~370 nm UV light of ~43μW/cm^2 power density. The transient response analysis gives the rise-time and fall-time characteristics of 4.20 s and 4.01 s of the proposed UV photodiode